Contents lists available at ScienceDirect
Automatica
journal homepage: www.elsevier.com/locate/automatica

Internal stability of dynamic quantised control for stochastic linear plants☆

Assaf Gurt, Girish N. Nair*

Department of Electrical and Electronic Engineering, University of Melbourne, VIC 3010, Australia

A R T I C L E   I N F O

Article history:
Received 20 May 2008
Received in revised form
12 November 2008
Accepted 9 February 2009
Available online xxxx

Keywords:
Quantized control
Stochastic control
Communication channels

A B S T R A C T

Existing analyses of 'zooming' quantisation schemes for bit-rate-limited control systems rely on the encoder and controller being initialised with identical internal states. Due to the quantiser discontinuity and the plant instability, it was not clear if closed-loop stability was possible if the encoder and controller commenced from different initial conditions. In this article, we consider partially observed, unstable linear time-invariant plants, with unbounded and possibly non-Gaussian noise, and propose a modified zooming-like scheme with finite-dimensional internal encoder and controller states that may not initially be identical. Using a stochastic pseudo-norm, we prove that this scheme yields mean-square stability in all closed-loop state variables, not just the plant state, under a sufficient condition involving this initial error, the plant dynamics and the channel data rate. With diminishing initial error, this condition approaches a known universal lower bound on data rates and becomes tight. Furthermore, we show that the scheme automatically corrects itself, in the sense that the errors between the internal states of the encoder and controller tend to zero stochastically with time. This suggests that the policy will maintain stability in the presence of channel errors, for sufficiently low bit error rates. We support these conclusions with simulations.

1. Introduction

Due to the rapid growth in communication technology over the last few years, it is becoming increasingly common to employ digital communication networks for the exchange of information in large control systems. Many applications have arisen in the broad areas of sensor networks, industrial automation, vehicular technology, irrigation and defence systems. Although the total capacity of the network may be large, each sensor or actuator may be allocated only a small portion, placing severe limitations on performance. This has recently led to a vast amount of research into the synthesis and analysis of control systems with communication-limited feedback — see the special issue Antsaklis and Baillieul (2007).

Our focus in this article is on systems in which this limitation takes the form of a digital channel carrying a finite number of bits per unit time. Despite notable theoretical advances, the subtle interplay between communications and control concepts and the technical challenge posed by the discontinuous nonlinearity of the channel, have made it difficult to answer many fundamental questions, even for the basic scenario of a centralised, linear time-invariant (LTI) plant stabilised over a single errorless channel.

The many coding and control schemes that have been proposed in this context can be broadly categorised according to whether or not the resolution and range of the quantiser (i.e. analogue-to-digital converter) depend on previous quantised values. For the case of unstable, noiseless LTI plants with bounded but unknown initial states, it was proven in Wong and Brockett (1999) and Baillieul (2001) that memoryless, static quantisers and controllers could ensure bounded plant states under certain conditions relating the data rate to the sampled plant dynamics. These conditions were tight for scalar plants.

The design of memoryless quantised controllers for noiseless LTI plants has been further studied in Ishii and Francis (2003) in terms of quadratic stability and in Li and Baillieul (2004, 2007) with regard to the robust and efficient use of channel data rate. In a recent article (Azuma & Sugie, 2008) on LTI plants with fixed, finite input sets, dynamic but fixed-resolution quantisation schemes similar to predictive quantisation and delta modulation in communications (Gersho & Gray, 1993) were proposed and studied.

Although the schemes above offer the advantage of simplicity, their finite quantiser resolution and range make asymptotic stability impossible and also retard their responses to large initial states. The fixed range also imposes an upper bound on the largest instantaneous magnitude of any additive process noise in the plant, above which boundability is lost. Indeed, with unbounded

☆ The material in this paper was partially presented at 17th IFAC World Congress, Seoul, Korea, July 6–11, 2008. This paper was recommended for publication in revised form by Associate Editor Andrey V. Savkin under the direction of Editor Ian R. Petersen.

* Corresponding author. Tel.: +61 3 83446701; fax: +61 3 83446678.
E-mail addresses: agurt@ee.unimelb.edu.au (A. Gurt), gnair@unimelb.edu.au (G.N. Nair).

0005-1098/$ – see front matter Crown Copyright © 2009 Published by Elsevier Ltd. All rights reserved.
doi:10.1016/j.automatica.2009.02.016

process noise and unstable plant dynamics, it has been shown that stochastic stability is impossible using a bounded quantisation range (Nair & Evans, 2004), since the unbounded noise and unstable plant dynamics will eventually push the quantiser input progressively deeper into the quantiser saturation region.

A solution to these shortcomings is to dynamically expand or contract ('zoom') the quantiser range according to the most recent quantiser output. Zooming quantisation was first studied in the communications literature, where it is called *adaptive* or *feedback* quantisation, with stationary or independent, identically distributed (iid) input signals typically assumed (Goodman & Gersho, 1974; Kieffer, 1982). The important articles (Brockett & Liberzon, 2000; Liberzon, 2003) contained the first formulation and analyses of such a scheme for unstable plants in a control loop and have been extended to accommodate process noise satisfying an unknown bound (Liberzon & Nesic, 2007). In Nair and Evans (2004), a zooming-like scheme was proposed and shown to mean-square-stabilise the states of a stochastic LTI plant at any data rate down to a universal infimum. In Fagnani and Zampieri (2004) a 'zooming'-like quantisation scheme for noiseless LTI plants was also investigated in terms of controller complexity versus performance.

Although the zooming quantised controllers discussed above possess their own internal states, only the stability properties of the plant state were analysed. Furthermore, these analyses relied heavily on the assumption that the internal encoder and controller states were initially known and identical, enabling the encoder to exactly determine how the controller state evolved with each transmitted bit. However, in practical channels the bit error rate (BER) will never be exactly zero, even with channel error correction coding. With probability arbitrarily close to 1, a bit will be received erroneously after a sufficiently long time, at which point the internal controller state will differ from what the encoder predicts. As previously noted in Nair and Evans (2004) (p. 431), given the unstable dynamics of the plant and the discontinuous, nonlinear nature of quantisation, it was unclear if closed-loop stability could be maintained even if this difference was arbitrarily small. For unstable LTI noiseless plants, this question is addressed in the recent article (Kameneva & Nesic, 2009).

In this article, we present a solution for the case of a stochastic LTI plant with unbounded process and measurement noise. No statistical structure is imposed on this noise beyond having a uniformly bounded higher moment; however, *a priori* knowledge of an upper bound on this moment is not required to establish stability. We present our formulation in Section 2, focusing on scalar plants initially, and construct in Section 3 a time-invariant, finite-dimensional, dynamic coding and control scheme. In Section 4, we prove that a stochastic functional introduced in Nair and Evans (2004) is a pseudo-norm and then use this to establish mean square stability in *all* closed-loop state variables, not just the plant state, under a sufficient condition on the channel data rate, the plant dynamics and certain parameters of the encoder and controller.

We then show in Section 5 the surprising result that the internal states of the encoder and controller asymptotically converge in mean absolute and proportional almost-sure senses. This suggests that the scheme may also be able to achieve stability over erroneous channels at sufficiently low BER's. In this context the time-invariance of our scheme is useful, since the encoder and controller do not know in advance when a bit error occurs. Though the important articles (Matveev & Savkin, 2007a,b) have provided rigorous, tight criteria for stabilisability over erroneous channels (albeit in almost-sure asymptotic and bounded senses, not mean-square), the constructions presented there require the random generation of long error-correction codes, unlike the case here. The idea of achieving immunity to channel errors by using an appropriately designed zooming quantiser was investigated in Goodman and Wilkinson (1975), in the context of encoding and decoding an iid process under an expected logarithm error criterion. In contrast, we consider the stronger objective of mean square stability and must also cope with the presence of feedback and unstable plant dynamics.

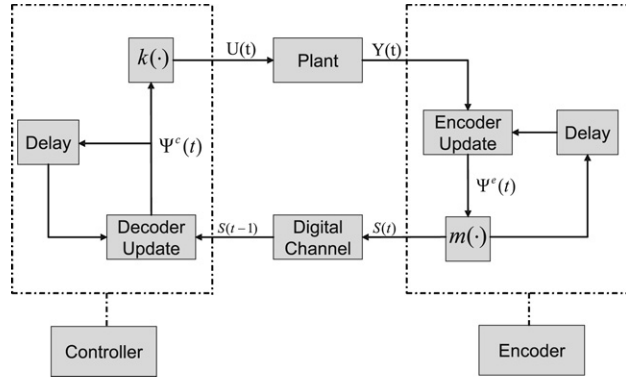

Fig. 1. Dynamic quantised control scheme.

In Section 6, we extend these results to multi-input multi-output plants with n-dimensional states, using the technique of down-sampling. Furthermore, we show that as the initial error between encoder and decoder states diminishes, the corresponding sufficient condition for stability approaches a known universal lower bound for mean square stabilisability in the plant state (49). Finally, simulation results supporting these conclusions are presented and discussed in Section 7.

2. Formulation

To begin with, consider the stochastic, scalar plant

$$X(t+1) = \lambda X(t) + bU(t) + V(t), \qquad Y(t) = cX(t) + W(t), \quad (1)$$

where $X(t), U(t), Y(t), V(t), W(t) \in \mathbb{R}$ are the plant state, input, output, process noise and measurement noise respectively and where $t \in \mathbb{Z}_{\geq 0}$. It is assumed that $b, c \neq 0$ and that

A1: $\exists$ a known $\varepsilon > 0$ s.t. $\mathrm{E}\{|X(0)|^{2+\varepsilon}\}$, $\sup_{t\geq 0} \mathrm{E}\{|V(t)|^{2+\varepsilon}\}$, $\sup_{t\geq 0} \mathrm{E}\{|W(t)|^{2+\varepsilon}\} < \infty$.

Remark. Bounded higher moment conditions such as A1 are also found in quantisation theory (Graf & Luschgy, 2000). They admit not only exponentially decaying distributions such as the Gaussian, but also distributions with 'fat' power-law tails.

As depicted in Fig. 1, the plant output $Y(t)$ is encoded into a *symbol* $S(t)$, which is transmitted over an errorless digital channel, decoded and then converted into a control input $U(t)$. The symbol $S(t)$ transmitted over the channel at time t is chosen from a finite and possibly time-varying alphabet $\mathcal{S}(t)$, with a finite (average) channel data rate

$$R := \liminf_{\tau\to\infty} \frac{1}{\tau} \sum_{t=0}^{\tau-1} \log_2 |\mathcal{S}(t)| < \infty \text{ (bits/sample)}. \quad (2)$$

The encoder and controller have their own, finite-dimensional internal states $\Psi^e(t) \in \mathbb{R}^e$ and $\Psi^c(t) \in \mathbb{R}^c$ respectively, which are updated recursively:

$$\left(\Psi^e(t-1), Y(t)\right) \mapsto \Psi^e(t), \qquad S(t) = m\left(\Psi^e(t)\right) \in \mathcal{S}(t) \quad (3)$$

$$\left(\Psi^c(t-1), S(t-1)\right) \mapsto \Psi^c(t), \qquad U(t) = k\left(\Psi^c(t)\right) \in \mathbb{R}. \quad (4)$$

We define a *finite-dimensional encoder-controller (FDEC)* by the alphabet sequence $\{\mathcal{S}(t)\}_{t=0}^{\infty}$ together with the finite-dimensional and possibly time-varying mappings (3)–(4). Examples of FDEC's include the *zooming* quantisers of Brockett and Liberzon (2000), Liberzon (2003), Fagnani and Zampieri (2004) and Liberzon and Nesic (2007) and the *finitely recursive* coding and control scheme of Wong and Brockett (1999), all proposed for linear time-invariant (LTI) plants with bounded or no noise, as well as the scheme of Nair and Evans (2004) for stochastic LTI plants with unbounded noise.

As discussed in Section 1, a critical assumption upon which the stability analyses of these previous schemes relied was that the initial internal states $\Psi^{\mathrm{e}}(0)$, $\Psi^{\mathrm{c}}(0)$ matched exactly, allowing the encoder to predict the controller internal states exactly if no transmission errors occur. Given the unstable dynamics of the plant and the discontinuous quantiser nonlinearity, it was unclear if closed-loop stability would be preserved if this initial match were not exact or if a symbol error were to occur in the channel.

In this paper, we construct a specific FDEC for the stochastic plant (1) and show that it ensures mean square stability in all closed-loop state variables, i.e.

$$\sup_{t\geq 0} \mathrm{E}\{|X(t)|^2\}, \sup_{t\geq 0} \mathrm{E}\{\|\Psi^{\mathrm{e}}(t)\|^2\}, \sup_{t\geq 0} \mathrm{E}\{\|\Psi^{\mathrm{c}}(t)\|^2\} < \infty,$$

under a criterion involving plant and FDEC parameters, the channel data rate and a known bound on the proportional error between the initial internal encoder and controller states (Theorem 3). Furthermore, we show that the internal states of the encoder and controller asymptotically 'resynchronise' with time (Theorem 5, Corollary 6), suggesting that stability may be maintained despite symbol errors in the channel (Section 7.2). We extend this FDEC to plants with n-dimensional states and show that in the limit of vanishing initial error, the sufficient criterion approaches the universal lower bound (49) for (mean-square) stabilisability and thus becomes tight (Theorem 7).

3. Stabilising scheme

In this section, we propose a specific time-invariant, finite-dimensional encoder-controller (FDEC) for the partially observed, stochastic plant (1).

Like the scheme proposed in Nair and Evans (2004), the FDEC here quantises a dynamically scaled error between the filtered plant state and the prediction based on the previous encoded state. However, since we no longer assume that the internal encoder and controller states match or that the encoder knows the exact control input, it turns out that the closed loop dynamics here are determined here by not just one but *three* coupled error terms – between the encoded and filtered plant state, between the decoded and encoded plant state and between the actual and filtered state – as well as three corresponding dynamic scaling factors. In addition, we permit a linear controller gain g, instead of a deadbeat-like law.

At time t, the internal encoder state is of the form

$$\Psi^{\mathrm{e}}(t) = \left(\hat{X}(t|t-1), X^{\mathrm{e}}(t), L^{\mathrm{e}}_G(t), L^{\mathrm{e}}_J(t), L^{\mathrm{e}}_H(t)\right) \in \mathbb{R}^2 \times \mathbb{R}^3_{>0}. \quad (5)$$

The first component, $\hat{X}(t|t-1)$, is a prediction of the plant state at time t given the outputs up to time $t-1$, the second component $X^{\mathrm{e}}(t)$ is the encoded state, and the last three components are dynamic scaling factors used to adjust the quantiser range. The first component is updated as

$$\hat{X}(t+1|t) = \lambda\hat{X}(t|t-1) + bgX^{\mathrm{e}}(t) + k^{\mathrm{o}}[Y(t) - c\hat{X}(t|t-1)]. \quad (6)$$

This is a linear Luenberger observer with gain k^{o}, but with one important difference: due to the uncertainty in the initial decoder internal state, the encoder *does not precisely know the control input* applied at time t and so approximates it by $gX^{\mathrm{e}}(t)$, g being the selected control gain.

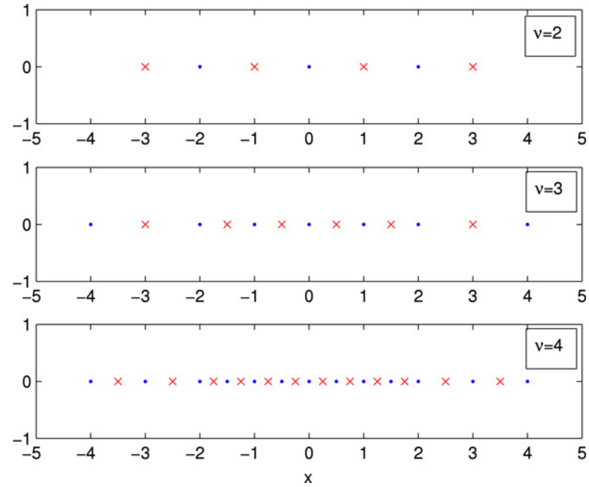

Fig. 2. Quantiser points and intervals ($\mu = 2$). Boundary points and quantiser points are denoted by '.' and 'x' respectively.

The second component, $X^{\mathrm{e}}(t)$ is updated according to a dynamic, predictive quantisation scheme, employing the non-uniform, oddly symmetric, static quantiser $q(\cdot)$ of Nair and Evans (2004) (pg. 425). For reasons of space we refer the reader to that article for a detailed discussion and analysis of its properties. Briefly, for given integers $\mu, \nu \geq 2$ and real $\varrho > \mu^{2/\varepsilon}$, $q(\cdot)$ acts by first partitioning the real line into $M = \mu^\nu$ non-uniform intervals as follows:

- $[-1, 1]$ is partitioned into $(\mu^2 - 2)\mu^{\nu-2}$ intervals of length $2/[(\mu^2-2)\mu^{\nu-2}]$,
- $\pm(\varrho^{i-2}, \varrho^{i-1}]$ are each partitioned into $(\mu-1)\mu^{\nu-i}$ intervals of length $(\varrho^{i-1} - \varrho^{i-2})/[(\mu-1)\mu^{\nu-i}]$, $\forall i \in [2, 3, \ldots, \nu]$,
- $\pm(\varrho^{\nu-1}, \infty)$ are left as the right- and left-most intervals.

These quantiser intervals are denoted $I(s)$, $s \in [0, \ldots, M-1]$, ordered from left- to right-most, and are finer closer to the origin and coarser, further away (see Fig. 2). Due to this nonuniformity, each $I(s)$ is associated with a *resolution* $\kappa(s)$, as well as a quantiser point $\varpi(s)$:

$$\kappa(s) := \begin{cases} \text{half-length of } I(s), & 1 \leq s \leq M-2 \\ \dfrac{\varrho - 1}{2 - 2/\mu}\varrho^{\nu-1}, & s \in \{0, M-1\} \end{cases} \quad (7)$$

$$\varpi(s) := \begin{cases} \text{midpoint of } I(s), & 1 \leq s \leq M-2, \\ \left(1 + \dfrac{\varrho-1}{2-2/\mu}\right)\varrho^{\nu-1}, & s = M-1, \\ -\left(1 + \dfrac{\varrho-1}{2-2/\mu}\right)\varrho^{\nu-1}, & s = 0. \end{cases} \quad (8)$$

$$q(x) := \varpi(s) \quad \text{if } x \in I(s). \quad (9)$$

At time t, the symbol transmitted is the unique index $S(t) \in [0, \ldots, M-1]$ of the quantised, dynamically scaled prediction error,

$$\varpi(S(t)) = q\left(\frac{\left[\hat{X}(t+1|t) - (\lambda + bg)X^{\mathrm{e}}(t)\right]}{L^{\mathrm{e}}(t)}\right). \quad (10)$$

The corresponding data rate is $R = \log_2 M = \nu \log_2 \mu$ bits/sample. The encoded plant state and scaling factor $L^{\mathrm{e}}(t)$ are then updated according to

$$X^{\mathrm{e}}(t+1) = (\lambda + bg)X^{\mathrm{e}}(t) + L^{\mathrm{e}}(t)\varpi(S(t)) \quad (11)$$

$$L^{\mathrm{e}}(t) = |\lambda|L^{\mathrm{e}}_G(t) + |k^{\mathrm{o}}c|L^{\mathrm{e}}_J(t) + |k^{\mathrm{o}}|d_W, \quad (12)$$

Please cite this article in press as: Gurt, A., & Nair, G. N. Internal stability of dynamic quantised control for stochastic linear plants. Automatica (2009), doi:10.1016/j.automatica.2009.02.016

$$L^e_G(t+1) = L^e(t)\kappa(S(t)) \tag{13}$$

$$L^e_J(t+1) = |\lambda - k^o c| L^e_J(t) + |bg| L^e_H(t) + d_V + |k^o| d_W \tag{14}$$

$$L^e_H(t+1) = |\lambda + bg| L^e_H(t) + \eta L^e(t)[1+\kappa(S(t))], \tag{15}$$

where $d_V, d_W, \eta > 0$ are *arbitrary* positive constants.

Note that (11)–(15) only explicitly depend on the current transmitted symbol and the previous value of $(X^e(t), L^e_G(t), L^e_J(t), L^e_H(t))$, and not directly on the filter output $\hat{X}$. Thus, at the other end of the channel, the controller can run an exact copy of these update laws, *but on its own internal state*

$$\Psi^c(t) := \left(X^c(t), L^c_G(t), L^c_J(t), L^c_H(t)\right) \in \mathbb{R} \times \mathbb{R}^3_{>0}. \tag{16}$$

It receives the symbol $S(t-1) \in [0, \ldots, \mu^\nu - 1]$ at time $t \geq 1$ (due to the delay in the channel) and then sets

$$X^c(t+1) = (\lambda + bg)X^c(t) + L^c(t)\varpi(S(t)), \tag{17}$$

$$L^c(t) = |\lambda| L^c_G(t) + |k^o c| L^c_J(t) + |k^o| d_W, \tag{18}$$

$$L^c_G(t+1) = L^c(t)\kappa(S(t)), \tag{19}$$

$$L^c_J(t+1) = |\lambda - k^o c| L^c_J(t) + |bg| L^c_H(t) + d_V + |k^o| d_W, \tag{20}$$

$$L^c_H(t+1) = |\lambda + bg| L^c_H(t) + \eta L^c(t)[1+\kappa(S(t))], \tag{21}$$

$$U(t) = gX^c(t). \tag{22}$$

Remark. The quantities $L^x_G(t), L^x_J(t)$ and $L^x_H(t)$ (x being 'e' or 'c') can be regarded as the nominal uncertainties associated with the errors

$$J(t) := \hat{X}(t|t-1) - X(t), \tag{23}$$

$$G(t) := X^e(t) - \hat{X}(t|t-1), \qquad H(t) := X^c(t) - X^e(t), \tag{24}$$

due to quantisation and noise. These uncertainties contribute dynamically to the quantiser scaling factor and the encoded/decoded state estimates via (11)–(12) and (17)–(18). As will be seen in the next section, the update rules (12)–(15) and (18)–(20) are designed to closely mimic the dynamics (31)–(33) of the corresponding terms (23)–(24).

4. Internal stability analysis

We prove here that the time-invariant, finite-dimensional encoder-controller (FDEC) (6)–(22) achieves internal mean square stability, in the sense that all closed-loop state variables have second moments that are uniformly bounded over time.

4.1. Pseudo-norm

The unbounded noise and quantiser nonlinearity make it difficult to directly obtain recursive bounds on mean square norms. Instead, we use a *pseudo-norm*

$$\|X, L\|_* := \sqrt{\mathrm{E}\left\{L^2 + |X|^{2+\varepsilon} L^{-\varepsilon}\right\}} \in [0, \infty], \tag{25}$$

defined on the space of random vectors $(X, L) \in \mathbb{R} \times \mathbb{R}_{>0}$.[1] This functional was introduced in Nair and Evans (2004) (p. 425). Though not observed there that it obeyed the triangle inequality (see Appendix A), it was however shown that

$$\|X, L\|^2_* \geq \mathrm{E}\{X^2\}, \mathrm{E}\{L^2\} \tag{26}$$

and that the errors produced by the quantisation mappings $q(\cdot)$ and $\kappa(\cdot)$ (7)–(8) satisfy

$$\left\| X - Lq\left(\frac{X}{L}\right), L\kappa(S) \right\|_* \leq \frac{\zeta}{\mu^\nu} \|X, L\|_*, \quad \forall \nu \in [2, 3, \ldots). \tag{27}$$

In the second bound, $\zeta > 0$ is a constant that depends on ε and the quantiser parameters μ, ϱ, but is *independent* of ν and the distribution of X, L. This independence, together with the appearance of $\|\cdot\|_*$ on both sides, allows it to be applied recursively to generate useful bounds.[2]

4.2. Stability analysis

We first establish the mean square stability of the error terms (23)–(24). For any $t \in \mathbb{Z}_{\geq 0}$, let

$$Z_G(t) := L^c_G(t) - L^e_G(t), \tag{28}$$

$$Z_J(t) := L^c_J(t) - L^e_J(t), \qquad Z_H(t) := L^c_H(t) - L^e_H(t), \tag{29}$$

$$F(t) := \max\left\{\frac{|Z_G(t)|}{L^e_G(t)}, \frac{|Z_J(t)|}{L^e_J(t)}, \frac{|Z_H(t)|}{L^e_H(t)}\right\}. \tag{30}$$

We have the following result:

Lemma 1 ($F(t)$ *Decreases Monotonically*). *Let the FDEC (5)–(22) be used on the plant (1). Then the maximum proportional scaling error (30) decreases monotonically to a limiting random variable $F_* \geq 0$ with time, whether or not the closed loop is stable.*

Proof. See Appendix B. □

From (1), (6), (11) and (17), as well as the even symmetry of the quantiser, it is straightforward to show that the coupled dynamics of the random errors (23)–(24) are given by

$$G(t+1) = \lambda G(t) + k^o cJ(t) - k^o W(t) - L^e(t) q\left(\frac{\lambda G(t) + k^o cJ(t) - k^o W(t)}{L^e(t)}\right) \tag{31}$$

$$J(t+1) = (\lambda - k^o c)J(t) - bgH(t) - V(t) + k^o W(t), \tag{32}$$

$$H(t+1) = (\lambda + bg)H(t) - \left(L^c(t) - L^e(t)\right) q \times \left(\frac{\lambda G(t) + k^o cJ(t) - k^o W(t)}{L^e(t)}\right). \tag{33}$$

Now define the non-random 3-vector

$$\beta(t) := \left[\|G(t), L^e_G(t)\|_*, \|J(t), L^e_J(t)\|_*, \|H(t), L^e_H(t)\|_*\right]^{\mathrm{T}}. \tag{34}$$

Pseudo-norm properties and the quantiser error bound (27) yield the following bound:

Lemma 2 (*Recursive Bound on Pseudo-Norm*). *Suppose the FDEC parameter η (15), (21) upper-bounds $F(0)$, the initial proportional scaling error (30). Then the error pseudo-norm vector (34) obeys the sublinear non-negative recursion*

$$\beta(t+1) \leq \Xi\beta(t) + \chi, \quad \forall t \geq 0, \tag{35}$$

component-wise, where $\chi \in \mathbb{R}^3_{\geq 0}$ is defined in (C.5) and

$$\Xi := \begin{bmatrix} \zeta|\lambda|\mu^{-\nu} & \zeta|k^o c|\mu^{-\nu} & 0 \\ 0 & |\lambda - k^o c| & |bg| \\ \eta|\lambda|\left(1 + \frac{\zeta}{\mu^\nu}\right) & \eta|k^o c|\left(1 + \frac{\zeta}{\mu^\nu}\right) & |\lambda + bg| \end{bmatrix}, \tag{36}$$

with ζ being the constant of (27).

[1] As the underlying space is not linear, 'pseudo-norm' is a slight abuse of common terminology.

[2] It can be shown that no quantiser can yield a similar bound in terms of root-mean square quantities; either ζ would be distribution-dependent, or the RHS would involve a higher moment of X (Graf & Luschgy, 2000), rendering it impossible to apply recursively.

Please cite this article in press as: Gurt, A., & Nair, G. N. Internal stability of dynamic quantised control for stochastic linear plants. Automatica (2009), doi:10.1016/j.automatica.2009.02.016

Proof. See Appendix C. □

This result enables us to derive a condition for internal mean square stability as follows. If Ξ (36) is Schur, i.e. has eigenvalues inside the open unit disc, then (35) yields uniformly bounded $\{\beta(t)\}$. By the pseudo-norm property (26), $\{G(t), J(t), H(t), L_G^e(t), L_J^e(t), L_H^e(t)\}$ are then mean-square bounded over time. Using (23)–(24) to rewrite the plant dynamics as

$$X(t+1) = (\lambda + bg)X(t) + bg[H(t) + J(t) + G(t)] + V(t) \quad (37)$$

and observing that $\{V(t)\}$ is uniformly mean-square bounded and $|\lambda + bg| < 1$, it follows that $\{X(t)\}$ is also uniformly mean-square bounded.

Now note from (23)–(24), (28)–(30) and Lemma 1 that $\hat{X}(t|t-1) = X(t) + J(t)$, $X^e(t) = X(t) + J(t) + G(t)$, $X^c(t) = X(t) + J(t) + G(t) + H(t)$ and that $L_x^c(t) \le (1+\eta)L_x^e(t)$, where the subscript '$x$' denotes any of '$G$', '$J$' or '$H$'. Thus $\{\hat{X}(t|t-1), X^e(t), X^c(t), L_G^c(t), L_J^c(t), L^c(t)\}$ are also mean square bounded over time. These conclusions are summarised below:

Theorem 3 (*Main Stability Criterion*). *Let the time-invariant, finite-dimensional encoder-controller (FDEC) (5)–(22) be used on the partially observed, unstable linear plant (1) having unbounded noise. Suppose that the FDEC parameter η (15), (21) upper-bounds the initial maximum proportional scaling error $F(0)$ (30) and that the matrix Ξ (36) is Schur.*

Then the plant state (1) and FDEC internal states (5), (16) are uniformly mean-square-bounded over time.

Remark. If Ξ is Schur, then $\Xi^t \to 0$. By the nonnegativity of Ξ, the diagonal elements $\zeta|\lambda|\mu^{-\nu}$, $|\lambda - k^o c|$ and $|\lambda + bg|$ must then all be < 1.

Looking at the matrix (36), observe that it becomes upper triangular as $\eta \to 0$. As the eigenvalues of a triangular matrix are just the diagonal elements and since eigenvalues vary continuously with matrix elements (Horn & Johnson, 1985), we immediately have the following, simpler corollary.

Corollary 4 (*Stability Criterion with Small $F(0)$*). *If the number of quantiser levels $\mu^\nu > \zeta|\lambda|$ and $|\lambda + bg|, |\lambda - k^o c| < 1$, then for sufficiently small $\eta > 0$, the FDEC (5)–(22) achieves mean-square stability in all closed-loop state variables, for any initial maximum proportional scaling error $F(0) \le \eta$.*

Remark. The sufficient condition $\mu^\nu > \zeta|\lambda|$ is stronger than given in Nair and Evans (2004) for mean-square-stabilisable plant states, due to the presence of the factor $\zeta > 1$ from (27). However, it is possible to approach the infimum average data rate $\max\{\log_2|\lambda|, 0\}$ of Nair and Evans (2004) by *down-sampling*; this is illustrated more generally for plants with n-dimensional states in Section 6.

5. Asymptotic agreement between encoder and controller

In this section, we show that since the time-invariant finite-dimensional encoder-controller (FDEC) proposed in this paper achieves stability, it automatically recovers with time from initial errors in the internal encoder and controller states (5), (16). This is an important requirement for implementation over practical channels with small but non-zero bit error rate; otherwise, the accumulation of successive bit errors would lead to instability.

Our first main result concerns the almost sure (a.s.), monotonic convergence to zero of the maximum proportional scaling error between the encoder and controller states:

Theorem 5 ($F(t) \to 0$ *a.s.*). *Suppose that the time-invariant, finite-dimensional encoder-controller (5)–(22) used on the plant (1) yields $\sup_{t\ge0} \mathrm{E}\{L_G^e(t)^2\}$, $\sup_{t\ge0} \mathrm{E}\{L_J^e(t)^2\}$ and $\sup_{t\ge0} \mathrm{E}\{L_H^e(t)^2\} < \infty$.*

Then the maximum proportional scaling error $F(t)$ (30) monotonically tends to 0 with time, almost surely.

Proof. See Appendix D. □

Remarks. This result suggests that the FDEC can be simplified by zeroing the parameter η of (15) and (21), the role of which is to bound $F(t)$. It further hints that the stability criterion of Theorem 3 may be too strong and that all that is required is for the diagonal elements of Ξ (36) to be < 1. However, establishing these conjectures rigorously is left for future work.

Note also that the uniform mean-square boundedness (MSB) required of the scaling factors in this result is guaranteed if the conditions of Theorem 3 are met.

Using Theorem 5, it is straightforward to show that the unnormalised error between encoder and controller states must also tend to 0 in the mean absolute sense:

Corollary 6 (*Mean Absolute Convergence*). *If in addition to the hypotheses of Theorem 5, $F(0)$ is bounded above and the controller gain k of (22) satisfies $|\lambda + bg| < 1$, then the errors $H(t)$ (24), $Z_G(t)$, $Z_J(t)$, $Z_H(t)$ (28)–(29) between the internal encoder and controller state variables converge to 0 mean absolutely with time.*

Proof. See Appendix E. □

Remark. Note that all the hypotheses required by this corollary are guaranteed by the conditions of Theorem 3. We conjecture that the internal state errors must also converge to zero in the stronger mean square sense, as suggested by the simulations of Section 7. However, proving this may require more stringent hypotheses, such as asymptotically stationary $L_G^e(t)$, $L_J^e(t)$ and $L_H^e(t)$ or uniform boundedness of a higher moment, and is also left for future investigation.

6. Minimum rate and multivariable plants via downsampling

We now extend the results of the preceding sections to deal with multi-input multi-output (MIMO) plants with n-dimensional states. Our approach is to diagonalise and *down-sample* the MIMO plant and then exploit controllability and observability to reduce it to n scalar stochastic plants with decoupled dynamics and control inputs. Through appropriate time-sharing between these scalar plants, the total average rate can be brought as close as pleased to the universal infimum of Nair and Evans (2004).

Consider the stochastic, discrete-time MIMO plant

$$X(t+1) = AX(t) + BU(t) + V(t), \qquad Y(t) = CX(t) + W(t), \quad (38)$$

where $X(t), V(t) \in \mathbb{R}^n$, $U(t) \in \mathbb{R}^m$, $Y(t), W(t) \in \mathbb{R}^p$ are the plant state, process noise, input, output and measurement noise respectively. Assume that

B1 (A, B) is reachable and (C, A), observable.
B2 A is unstable, i.e. has spectral radius ≥ 1, and is diagonalisable with real eigenvalues.
B3 For some $\varepsilon > 0$, $\mathrm{E}\{\|X(0)\|^{2+\varepsilon}\}$, $\sup_{t\ge0} \mathrm{E}\{\|V(t)\|^{2+\varepsilon}\}$, $\sup_{t\ge0} \mathrm{E}\{\|W(t)\|^{2+\varepsilon}\} < \infty$.

Remark. Dropping either the assumptions of diagonalisability or the realness of eigenvalues in B2 would not change the results below but would necessitate explicit consideration of the real Jordan form of the matrix, resulting in a more complicated encoder-controller.

Without loss of generality (wlog), suppose a real similarity transformation matrix has been applied to the plant state $X(t)$ so that the matrix A is in diagonal form. For some sufficiently large integer $\tau \geq 2n$, let the time axis be divided up into *cycles* $[j\tau, \dots, (j+1)\tau - 1]$ of duration τ. The first n instants $t \in [j\tau, \dots, j\tau + n - 1]$ of each cycle constitute the *estimation phase*, during which the state $X(j\tau)$ at the start of the cycle is estimated. The last n instants, constituting the *control phase*, are the only times at which control inputs $U(t)$ are applied. The period in between is called the *transmission phase* and is described in more detail later.

Over the estimation phase, the plant outputs may be written

$$\tilde{Y}(j) = \mathbf{O}X(j\tau) + N(j), \tag{39}$$

where

$$\tilde{Y}(j) := \left[Y(j\tau + n - 1)^{\mathrm{T}}, \dots, Y(j\tau)^{\mathrm{T}}\right]^{\mathrm{T}} \in \mathbb{R}^{pn}, \tag{40}$$

$$\mathbf{O} := \left[(CA^{n-1})^{\mathrm{T}}, (CA^{n-2})^{\mathrm{T}}, \dots, C^{\mathrm{T}}\right]^{\mathrm{T}} \in \mathbb{R}^{pn \times n}, \tag{41}$$

$$N(j) := \begin{bmatrix} W(j\tau + n - 1) + \sum_{i=0}^{n-2} CA^{n-2-i}V(j\tau + i) \\ W(j\tau + n - 2) + \sum_{i=0}^{n-3} CA^{n-3-i}V(j\tau + i) \\ \vdots \\ W(j\tau) \end{bmatrix}. \tag{42}$$

By the observability of (C, A), the matrix $\mathbf{O}$ (41) has full column rank n and consequently a $n \times np$ pseudo-inverse $\mathbf{O}^*$. Multiplying (39) by $\mathbf{O}^*$, we obtain

$$Y'(j) := \mathbf{O}^*\tilde{Y}(j) = X(j\tau) + W'(j), \tag{43}$$

where $W'(j) := \mathbf{O}^*N(j)$. Next looking at the dynamics of the plant state from time $j\tau$ to $(j+1)\tau$, observe that

$$X'(j+1) := X((j+1)\tau) \equiv A^{\tau}X'(j) + U'(j) + V'(j), \tag{44}$$

where

$$U'(j) := \sum_{i=0}^{n-1} A^{i}BU((j+1)\tau - 1 - i), \tag{45}$$

$$V'(j) := \sum_{i=0}^{\tau-1} A^{\tau-1-i}V(j\tau + i). \tag{46}$$

The controllability of (A, B) is equivalent to any desired value of $u'(j) \in \mathbb{R}^n$ being implementable by suitable choice of inputs $\{u(t)\}_{t=(j+1)\tau-n}^{(j+1)\tau-1}$ in (45). Further noting that A is in diagonal form $\equiv \mathrm{diag}(\lambda_1, \dots, \lambda_n)$, we may pair the h-th components of (44), (43) to obtain n virtual scalar plants

$$X_h'(j+1) = \lambda_h^{\tau}X_h'(j) + U_h'(j) + V_h'(j) \in \mathbb{R}, \tag{47}$$

$$Y_h'(j) = X_h'(j) + W_h(j) \in \mathbb{R}, \tag{48}$$

with decoupled dynamics, outputs and control inputs. Furthermore the noise terms $V_h'(j), W_h'(j)$, being fixed linear functions of $\{V(t), W(t)\}_{t=j\tau}^{(j+1)\tau}$, have $(2+\varepsilon)$-th moments that are uniformly bounded over j. As these virtual plants are in the form (1) and satisfy assumptions A1, we may use the time-invariant, finite-dimensional encoder-controller (FDEC) (5)–(22) on each h-th plant, setting $\nu = \tau_h \geq 1, \lambda = \lambda_h^{\tau}, b = c = 1$. (Note that although the parameters d_V, d_W are arbitrary, for improved performance they should be of the same order as the root-mean $(2+\varepsilon)$-th power of the respective noise terms $V_h'(j), W_h(j)$.)

The protocol for allocating channel access to each virtual plant encoder is essentially the same as in Nair and Evans (2004) (sec. 5.2.2). In that article it was shown that in order to be able to mean square stabilise the states of a stochastic LTI plant with some causal, error-free encoder-controller, it is necessary and sufficient for the average data rate to satisfy

$$R > H := \sum_{h=1}^{n} \max\{\log_2 |\lambda_h|, 0\}, \tag{49}$$

where H is the *intrinsic entropy rate* of the plant. Pick any nominal data rate $R' > H$, select an integer $\mu \geq \max\{2, 2^{R'}\}$ and divide up the transmission phase $[j\tau + n, \dots, (j+1)\tau - n - 1]$ into $n+1$ *transmission slots*, with the h-th slot having duration τ_h. The $n+1$-th slot is idle, with nothing transmitted. During the h-th slot, where $h \leq n$, the h-th component of (47) with output (48) is encoded by the FDEC above and transmitted as a τ_h-length codeword with letters in a μ-ary alphabet. It can be shown that the choice of slot durations

$$\tau_h = \lfloor \log_{\mu} \max\{\zeta|\lambda_h|^{\tau}, 0\} \rfloor + 1, \quad \forall h \in [1, \dots, n], \tag{50}$$

(1) is feasible for large τ, i.e. $\sum_{h=1}^{n} \tau_h \leq \tau - 2n$,
(2) has average data rate $R = \sum_{h=1}^{n} \tau_h \log_2 \mu/\tau \leq R'$ for large τ,
(3) satisfies $\mu^{\tau_h} > \zeta|\lambda_h^{\tau}|$.

Thus if we select the controller and observer gains g, k^{o} for each virtual plant to satisfy $|\lambda_h^{\tau} + g|, |\lambda_h^{\tau} - k^{\mathrm{o}}| < 1$ then Corollary 4, Theorem 5 and Corollary 6 immediately yield the following result:

Theorem 7 (*Stability and Convergence for MIMO Plants*). *Suppose that the τ-periodically time-varying, finite-dimensional encoder-controller (FDEC) of this section is applied to the multi-input, multi-output stochastic plant (38).*

Then for sufficiently small $\eta > 0$ and any initial maximum proportional scaling error (30) $F(0) \leq \eta$, all closed-loop state variables are uniformly mean square bounded. Furthermore, the maximum proportional scaling errors monotonically $\to 0$ almost surely with time and the unnormalised errors between the encoder and controller states $\to 0$ mean absolutely.

Remark. Although the argument presented above only deals explicitly with the the states at times $t = j\tau$, the linear-time-invariance of the plant can be used to establish mean-square boundedness at all times t. The FDEC internal states of course only change at times $t = j\tau$.

7. Simulation results

In this section, we present Matlab simulations that illustrate the internal stability and asymptotic agreement results of Sections 4–5 for a noiseless digital channel. We then examine the effect of transmitting the quantiser outputs over a binary symmetric channel (BSC) with a non-zero bit error rate (BER).

We consider an unstable scalar plant (1), with parameters $\lambda = 1.1$, $b = c = 1$ and having independent Gaussian initial state, process and observation noise with mean 0 and variance 1. We set $\mu = 2$, $\nu = 2$ in the quantiser law (10) so that it has $\mu^{\nu} = 4$ levels, yielding a data rate of 2 bits/sample. In the finite-dimensional encoder-controller (FDEC) update rules (6) and (11)–(22), we set the parameters $g = -1.1$ and $k^{\mathrm{o}} = d_W = d_V = 1$. We initialise the encoder internal state (5) with the values $\hat{X}(0|-1) = 0$, $X^{\mathrm{e}}(0) = 100$, $L_G^{\mathrm{e}}(0) = 101$, $L_J^{\mathrm{e}}(0) = L_H^{\mathrm{e}}(0) = 1$ and the controller internal state (16) with $X^{\mathrm{c}}(0) = 0$, $L_G^{\mathrm{c}}(0) = L_J^{\mathrm{c}}(0) = L_H^{\mathrm{c}}(0) = 1$. Note the large initial errors $X^{\mathrm{e}}(0) - X^{\mathrm{c}}(0) = L_G^{\mathrm{e}}(0) - L_G^{\mathrm{c}}(0) = 100$. The simulations illustrated here were done over 100 time steps, with the squared states and errors at each time averaged over 1000 samples.

Please cite this article in press as: Gurt, A., & Nair, G. N. Internal stability of dynamic quantised control for stochastic linear plants. Automatica (2009), doi:10.1016/j.automatica.2009.02.016

7.1. Noiseless digital channel

Graphs (1) and (2) in Fig. 3 show that the plant has been successfully stabilised via a noiseless channel, with the FDEC parameter η of (15) and (21) set to 0 and 0.1 respectively. The average value of the squared plant state $X(t)^2$ roughly settles to around 100 in the former but to around 350 in the latter, with larger transients as well. This suggests that the performance of the system is highly affected by the parameter η. Indeed, since η serves as an upper bound on the proportional scaling error $F(t)$ (30) which monotonically $\rightarrow 0$ a.s., $\eta = 0$ may be optimal. A rigorous analysis of this conjecture is left for future work.

Graphs (3) and (4) in Fig. 4 show that the difference between $L_G^e(t)$ and $L_G^c(t)$ tends to zero in mean square and proportional senses respectively. This supports the analysis in Section 5.

7.2. Binary symmetric channel (BSC)

Fig. 5 illustrates the effect on average squared plant states when the 4-valued quantiser index $S(t)$ of (10) is transmitted as a 2-bit symbol over a BSC with probability of bit error or BER $P_e > 0$. This yields a probability of received *symbol* error of $1-(1-P_e)^2 \approx 2P_e$. The plant and FDEC parameters and initial states are otherwise all the same as in Section 7.1 and we set $\eta = 0$.

Observe in graph (5) that when $P_e = 0.01$, the average squares states still remain bounded over time despite bit errors (note: in digital communications, 0.01 is typically regarded as a high BER). We do not explicitly analyse the reasons for this here, but the intuitive explanation is related to the fact that, from Section 5, the difference between the FDEC encoder and controller states decreases towards zero between successive bit errors. If the speed of this decay is sufficiently fast compared to the mean time interval $\approx 1/(2P_e) = 50$ between successive symbol errors, then on average the system has sufficient time to recover before the next symbol error occurs. However, when P_e is increased from 0.01 to 0.045, graph (6) indicates that stability is lost; i.e. the mean time between successive symbol errors, which is now $\approx 1/(2 \times 0.045) = 11.1$, is too short to allow the encoder and controller to adequately resynchronise their states.

Remark. More thorough analyses of stabilisability over erroneous digital channels such as in Matveev and Savkin (2007a) and Matveev and Savkin (2007b) provide necessary and sufficient conditions that relate various information-theoretic notions of channel capacity to the intrinsic entropy rate H (49) of the plant. However, the sufficiency of these criteria was generally proven by using long, randomly generated channel error correction codes. In contrast, the scheme here is explicitly defined, finite-dimensional and does not require any error correction coding. The reason for this simplicity lies in the fact that each channel bit error results in an incorrect control input, which feeds through the unstable, noisy LTI plant to produce a statistically large output that a zooming-like encoder can automatically recapture, if appropriately designed.

In connection with this, note that bit errors in digital point-to-point channels often arise from a limited signal-to-noise ratio (SNR) in the physical layer. It has been established that, if the physical channel noise and plant noise are uncorrelated and additive Gaussian, then mean square stability can be achieved using linear analog transmitters and controllers, without digital coding and at any SNR corresponding to a channel capacity exceeding H (Braslavsky, Middleton, & Freudenberg, 2007; Freudenberg, Middleton, & Solo, 2006). The scheme proposed here raises the question of whether finite-dimensional schemes may also be able to achieve stability at erroneous channel information rates down to this infimum, when the transmission format is constrained to be digital. A detailed investigation of this question is left as future work.

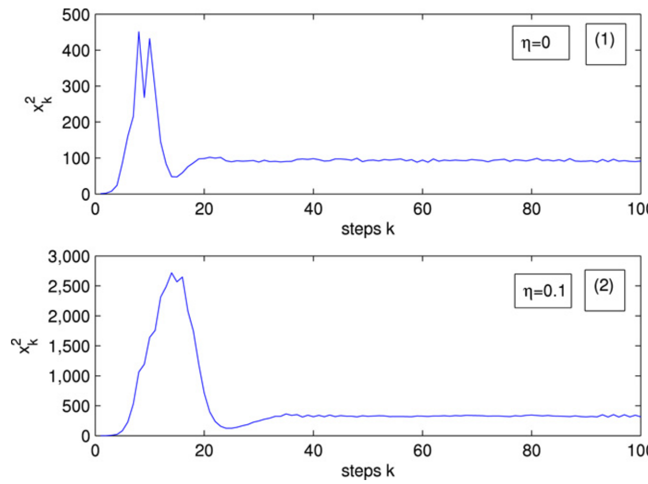

Fig. 3. Mean square stability.

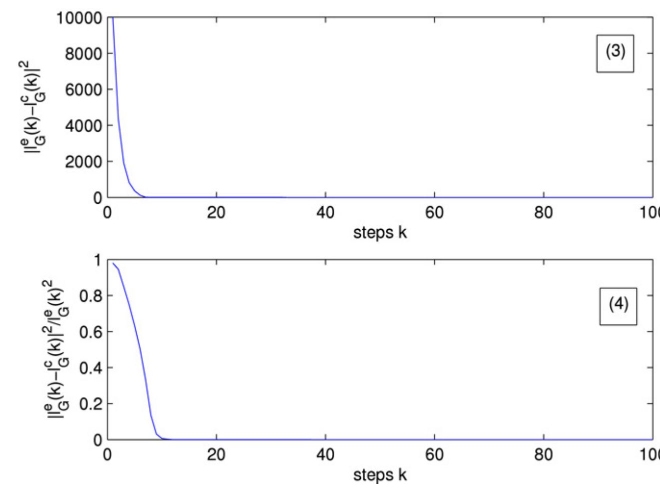

Fig. 4. Asymptotic agreement in mean-square and proportional almost-sure senses — convergence to zero.

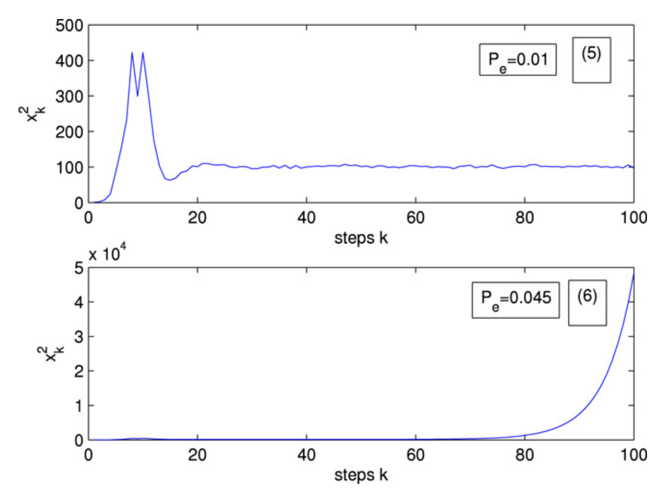

Fig. 5. Binary symmetric channel.

Acknowledgements

The authors acknowledge insightful discussions on this topic with colleagues Dr. T. Kameneva and Prof. D. Nesic at Uni. Melbourne.

Please cite this article in press as: Gurt, A., & Nair, G. N. Internal stability of dynamic quantised control for stochastic linear plants. Automatica (2009), doi:10.1016/j.automatica.2009.02.016

The authors gratefully acknowledge the financial support of the Dept. Education, Science and Training, National ICT Australia Ltd.'s Victoria Research Laboratory and Australian Research Council grant DP0664317.

Appendix A. Pseudo-norm properties

In addition to (26)–(27), the non-negative functional (25) has the following useful properties:

(1) Positive homogeneity:

$$\|dX, dL\|_* = d\|X, L\|_*, \quad \forall d > 0. \tag{A.1}$$

(2) Triangle inequality: ∀ random variables $X_1, X_2 \in \mathbb{R}, L_1, L_2 \geq 0$,

$$\|X_1 + X_2, L_1 + L_2\|_* \leq \|X_1, L_1\|_* + \|X_2, L_2\|_*. \tag{A.2}$$

These properties imply that $\|\cdot,\cdot\|_*$ is a *pseudo-norm* on the space of random vectors in $\mathbb{R} \times \mathbb{R}_{\geq 0}$.[3]

Property 1 is trivial, while the proof of Property 2 is as follows. Let $f(x) := \sqrt{1 + x^{2+\varepsilon}}$, $\forall x \geq 0$, noting that $\|X, L\|_*^2 \equiv \mathrm{E}\{L^2 f(|X|/L)^2\}$. It is straightforward to establish that f is convex and increasing, thus

$$\begin{aligned}
&(L_1+L_2) f\left(\frac{|X_1+X_2|}{L_1+L_2}\right) \leq (L_1+L_2) f\left(\frac{|X_1|+|X_2|}{L_1+L_2}\right) \\
&= (L_1+L_2) f\left(\frac{L_1}{L_1+L_2}\frac{|X_1|}{L_1} + \frac{L_2}{L_1+L_2}\frac{|X_2|}{L_2}\right) \\
&\leq (L_1+L_2)\left[\frac{L_1}{L_1+L_2} f\left(\frac{|X_1|}{L_1}\right) + \frac{L_2}{L_1+L_2} f\left(\frac{|X_2|}{L_2}\right)\right] \\
&= L_1 f\left(\frac{|X_1|}{L_1}\right) + L_2 f\left(\frac{|X_2|}{L_2}\right).
\end{aligned}$$

Squaring both sides and taking expectations,

$$\begin{aligned}
&\|X_1+X_2, L_1+L_2\|_*^2 \\
&\leq \|X_1, L_1\|_*^2 + \|X_2, L_2\|_*^2 + 2\mathrm{E}\left\{L_1 f\left(\frac{|X_1|}{L_1}\right) L_2 f\left(\frac{|X_2|}{L_2}\right)\right\} \\
&\leq \|X_1, L_1\|_*^2 + \|X_2, L_2\|_*^2 \\
&\quad + \sqrt{\mathrm{E}\left\{L_1^2 f\left(\frac{|X_1|}{L_1}\right)^2\right\}}\sqrt{\mathrm{E}\left\{L_2^2 f\left(\frac{|X_2|}{L_2}\right)^2\right\}} \\
&\equiv \left(\|X_1, L_1\|_* + \|X_2, L_2\|_*\right)^2,
\end{aligned} \tag{A.3}$$

where (A.3) follows from the Cauchy–Schwarz inequality. Taking square roots then yields (A.2). □

Appendix B. Proof of Lemma 1 (Monotonic decrease of maximum proportional scaling error)

Subtracting $L_G^e(t+1)$ (13) from $L_G^c(t+1)$ (19) and using the definition of $Z_G(t)$ (28), we obtain

$$\begin{aligned}
Z_G(t+1) &= |\lambda| Z_G(t) + |k^o c| Z_J(t) \\
&= |\lambda| L_G^e(t)\frac{Z_G(t)}{L_G^e(t)} + |k^o c| L_J^e(t)\frac{Z_J(t)}{L_J^e(t)}.
\end{aligned}$$

Applying moduli, the triangle inequality and the definition of $F(t)$ (30), we obtain

$$\begin{aligned}
|Z_G(t+1)| &\leq [|\lambda| L_G^e(t) + |k^o c| L_J^e(t)] F(t) \\
&\equiv [L_G^e(t+1) - |k^o| d_W] F(t)
\end{aligned}$$

$$\Leftrightarrow \frac{|Z_G(t+1)|}{L_G^e(t+1)} \leq \left(1 - \frac{|k^o| d_W}{L_G^e(t+1)}\right) F(t) < F(t). \tag{B.1}$$

Similarly, (14)–(15), (20)–(21) and (29)–(30) yield

$$\frac{|Z_J(t+1)|}{L_J^e(t+1)} \leq \left(1 - \frac{d_V + |k^o| d_W}{L_J^e(t+1)}\right) F(t) < F(t), \tag{B.2}$$

$$\frac{|Z_H(t+1)|}{L_H^e(t+1)} \leq \left(1 - \frac{\eta |k^o| d_W}{L_H^e(t+1)}\right) F(t) < F(t). \tag{B.3}$$

Taking the maximum of (B.1)–(B.3) and using definition (30) again, we see that

$$F(t+1) < F(t), \tag{B.4}$$

i.e. $\{F(t)\}$ is a decreasing sequence. As it is bounded below by 0, it must therefore converge monotonically to a limit $F_* \geq 0$, for each realisation of noise and initial state. □

Appendix C. Proof of Lemma 2 (recursive bound on error pseudo-norms)

Observe that $G(t+1)$ (31) is the error between $E(t) := \lambda G(t) + k^o J(t) - k^o W(t)$ and its quantised value. Applying the pseudo-norm to it and the corresponding scaling factor $L_G^e(t+1)$ (13), the bound (27) yields

$$\begin{aligned}
&\|G(t+1), L_G^e(t+1)\|_* \\
&= \left\|E(t) - L^e(t) q\left(\frac{E(t)}{L^e(t)}\right), L^e(t)\kappa(S(t))\right\|_* \\
&\overset{(27)}{\leq} \frac{\zeta}{\mu^\nu}\|E(t), L^e(t)\|_* \\
&\overset{(A.2),(A.1)}{\leq} \frac{\zeta}{\mu^\nu}\left(|\lambda| \|G(t), L_G^e(t)\|_* + |k^o c| \|J(t), L_J^e(t)\|_*\right. \\
&\quad \left. + |k^o| \|W(t), d_W\|_*\right).
\end{aligned} \tag{C.1}$$

Similarly, applying $\|\cdot,\cdot\|_*$ to (32), (14) gives

$$\begin{aligned}
&\|J(t+1), L_J^e(t+1)\|_* \overset{(A.2),(A.1)}{\leq} |\lambda - k^o c| \|J(t), L_J^e(t)\|_* \\
&\quad + |bg| \|H(t), L_H^e(t)\|_* + \|V(t), d_V\|_* + |k^o| \|W(t), d_W\|_*.
\end{aligned} \tag{C.2}$$

Now, by Lemma 1,

$$\begin{aligned}
&\eta \geq |Z_G(t)|/L_G^e(t), |Z_J(t)|/L_J^e(t), \quad \forall t \geq 0. \\
&\Rightarrow |L^c(t) - L^e(t)| = \left||\lambda| Z_G(t) + |k^o c| Z_J(t)\right| \\
&\qquad \leq \eta\left(|\lambda| L_G^e(t) + |k^o c| L_J^e(t)\right) < \eta L^e(t).
\end{aligned}$$

Taking the modulus of (33) and applying this, we obtain

$$\begin{aligned}
|H(t+1)| &< |\lambda + bg| |H(t)| + \eta L^e(t)\left|q\left(\frac{E(t)}{L^e(t)}\right)\right| \\
&< |\lambda + bg| |H(t)| + \eta(|N(t)| + |E(t)|),
\end{aligned} \tag{C.3}$$

where $N(t)$ is the quantisation error

$$N(t) := L^e(t) q\left(\frac{E(t)}{L^e(t)}\right) - E(t).$$

[3] To be a norm, we would also need $\|X, L\|_* = 0 \Leftrightarrow X, L = 0$ a.s.. The bound (26) establishes the forward implication, but the reverse is false: if we constrain $L = |X|^{1+2/\varepsilon}$, then $\|X, L\|_* \geq 1$ even if $X = L = 0$ a.s.

Applying the pseudo-norm to (C.3) and $L_H^e(t)$ (15) and noting that $\|\cdot,\cdot\|_*$ is increasing in the 1st argument modulus,

$$\|H(t+1), L_H^e(t+1)\|_* \overset{(A.2),(A.1)}{\leq} |\lambda + bg|\|H(t), L_H^e(t)\|_* + \eta\|N(t), L^e(t)\kappa(t)\|_* + \eta\|E(t), L^e(t)\|_*$$
$$\overset{(27)}{\leq} |\lambda + bg|\|H(t), L_H^e(t)\|_* + \eta\left(\frac{\zeta}{\mu^\nu}+1\right)\|E(t), L^e(t)\|_*$$
$$\overset{(A.2)}{\leq} |\lambda + bg|\|H(t), L_H^e(t)\|_* + \eta\left(\frac{\zeta}{\mu^\nu}+1\right)\Big(|\lambda|\|G(t), L_G^e(t)\|_* + |k^o c|\|J(t), L_J^e(t)\|_* + |k^o|\|W(t), d_W\|_*\Big). \quad \text{(C.4)}$$

Let $\bar{w}, \bar{v} < \infty$ be upper bounds on $\|W(t), d_W\|_*$, $\|V(t), d_V\|_*$ respectively, noting that these pseudo-norms are uniformly bounded since $W(t), V(t)$ are uniformly bounded in $(2+\varepsilon)$-th moment (assumptions A1). Combining (C.1), (C.2) and (C.4), we obtain the recursion (34), where

$$\chi := \left[\zeta|k^o|\mu^{-\nu}\bar{w}, \bar{v} + |k^o|\bar{w}, \eta(1+\zeta\mu^{-\nu})|k^o|\bar{w}\right]^{\mathrm{T}}. \quad \square \quad \text{(C.5)}$$

Appendix D. Proof of Theorem 5 (Proportional scaling errors → 0 a.s.)

The proof is by contradiction. By Lemma 1, $F(t)$ decreases monotonically to a limiting random variable $F_* \geq 0$. Suppose that this is not a.s. 0, i.e. that $\Pr\{F_* > 0\} > 0$. Taking the maximum of (B.1)–(B.3),

$$F(t+1) \leq \max\left\{1 - \frac{|k^o|d_W}{L_G^e(t+1)}, 1 - \frac{d_V + |k^o|d_W}{L_J^e(t+1)}, 1 - \frac{\eta|k^o|d_W}{L_H^e(t+1)}\right\} F(t).$$

Taking inferior limits,

$$F_* \leq \liminf_{t\to\infty} \max\left\{1 - \frac{|k^o|d_W}{L_G^e(t+1)}, 1 - \frac{d_V + |k^o|d_W}{L_J^e(t+1)}, 1 - \frac{\eta|k^o|d_W}{L_H^e(t+1)}\right\} \underbrace{\limsup_{t\to\infty} F(t)}_{=F_*} \quad \text{a.s.}.$$

$$\Rightarrow 1 \leq \liminf_{t\to\infty} \max\left\{1 - \frac{|k^o|d_W}{L_G^e(t+1)}, 1 - \frac{d_V + |k^o|d_W}{L_J^e(t+1)}, 1 - \frac{\eta|k^o|d_W}{L_H^e(t+1)}\right\} \quad \text{(D.1)}$$
$$= 1 - \limsup_{t\to\infty} \min\left\{\frac{|k^o|d_W}{L_G^e(t+1)}, \frac{d_V + |k^o|d_W}{L_J^e(t+1)}, \frac{\eta|k^o|d_W}{L_H^e(t+1)}\right\}, \quad \text{w.p.} > 0, \quad \text{(D.2)}$$

where (D.1) is obtained by dividing through by F_*, which > 0 with probability (w.p.) > 0. As the superior limit in (D.2) is nonnegative, it must then $= 0$, w.p. > 0. Defining

$$L(t) := \max\left\{\frac{L_G^e(t)}{|k^o|d_W}, \frac{L_J^e(t)}{d_V + |k^o|d_W}, \frac{L_H^e(t)}{\eta|k^o|d_W}\right\}, \quad \text{(D.3)}$$

this implies $\liminf_t L(t) = \infty$ w.p. >0. That is, $\exists\phi > 0$ s.t.

$$\phi < \Pr\{\liminf_{t\to\infty} L(t) = \infty\} = \Pr\{\sup_{t\geq 0}\inf_{s\geq t} L(s) = \infty\}$$
$$= \Pr\left\{\cap_{n\geq 1}\cup_{t\geq 0}\cap_{s\geq t} A_{n,s}\right\}$$
$$\leq \Pr\left\{\cup_{t\geq 0}\cap_{s\geq t} A_{n,s}\right\} = \sup_{t\geq 0}\Pr\left\{\cap_{s\geq t} A_{n,s}\right\}, \quad \forall n \geq 1, \quad \text{(D.4)}$$

where $A_{n,s}$ denotes the event $\{L(s) \geq n\}$ and where the last equality is due to the fact that $\cap_{s\geq t} A_{n,s}$ expands with t. Thus $\forall n \geq 1$, $\exists t_n$ sufficiently large that

$$\phi < \Pr\{\cap_{s\geq t_n} A_{n,s}\} \leq \Pr\{A_{n,t_n}\} = \Pr\{L(t_n) > n\}. \quad \text{(D.5)}$$

However, by the mean square boundedness of the scaling factors, $\exists\theta < \infty$ s.t. $\forall t \geq 0$,

$$\theta \geq \mathrm{E}\left\{\left|\frac{L_G^e(t)}{|k^o|d_W}\right|^2 + \left|\frac{L_J^e(t)}{d_V + |k^o|d_W}\right|^2 + \left|\frac{L_H^e(t)}{\eta|k^o|d_W}\right|^2\right\} \overset{(D.3)}{\geq} \mathrm{E}\{L(t)^2\}.$$

By the Chebychev inequality $\Pr\{L(t) > n\} \leq \theta n^{-2}$, $\forall n \geq 1, t \geq 0$. Thus $\forall n \geq \sqrt{2c/\phi}$, $t \geq 0$, we have $\Pr\{L(t) > n\} \leq \phi/2$, contradicting (D.5). $\square$

Appendix E. Proof of Corollary 6 (Asymptotic mean absolute agreement)

Let $\sup_{t\geq 0}\mathrm{E}\{L_x^e(t)^2\} =: \theta < \infty$, where the subscript '$x$' denotes either '$G$', '$J$' or '$H$'. We have

$$\mathrm{E}\{|Z_x(t)|\} = \mathrm{E}\left\{\frac{|Z_x(t)|}{L_x^e(t)}L_x^e(t)\right\} \overset{(30)}{\leq} \mathrm{E}\{F(t)L_x^e(t)\}$$
$$\leq \sqrt{\mathrm{E}\{F(t)^2\}\mathrm{E}\{L_x^e(t)^2\}} \leq \sqrt{\theta\mathrm{E}\{F(t)^2\}},$$

where we have used the Cauchy–Schwarz inequality (p. 276) in the last line. As $\eta^2 \geq F(t)^2 \to 0$ a.s., Lebesgue's dominated convergence theorem guarantees that the RHS $\to 0$. Hence $\mathrm{E}\{|Z_x(t)|\} \to 0, \forall$ 'x' $\in$ {'G', 'J','H'}.

Writing $L^e(t) - L^c(t) \equiv \lambda Z_G(t) + k^o c Z_J(t)$ in (33), applying moduli and taking expectations,

$$\mathrm{E}\{|H(t+1)|\} \leq |\lambda + bg|\mathrm{E}\{|H(t)|\} + \big(|\lambda|\mathrm{E}\{|Z_G(t)|\} + |k^o c|\mathrm{E}\{|Z_J(t)|\}\big)\bar{q},$$

where $\bar{q}$ is an upper bound on $|q(\cdot)|$. As $|\lambda + bg| < 1$ and $\mathrm{E}\{|Z_G(t)|\}, \mathrm{E}\{|Z_J(t)|\} \to 0$, it follows that $\mathrm{E}\{|H(t)|\} \to 0$. $\square$

References

Antsaklis, P, & Baillieul, J. (2007). Technology of networked control systems. *Proceedings of the IEEE*, *95* (1) (special issue).

Azuma, S., & Sugie, T. (2008). Optimal dynamic quantizers for discrete-valued input control. *Automatica*, *44*, 396–406.

Baillieul, J. (2001). Feedback designs in information-based control. In B. Pasik-Duncan (Ed.), *Stochastic theory and control proceedings of a workshop held in Lawrence, Kansas* (pp. 35–57). Springer.

Braslavsky, J. H., Middleton, R. H., & Freudenberg, J. S. (2007). Feedback stabilization over signal-to-noise ratio constrained channels. *IEEE Transactions on Automatic Control*, *52*(8), 1391–1403.

Brockett, R. W., & Liberzon, D. (2000). Quantized feedback stabilization of linear systems. *IEEE Transactions on Automatic Control*, *45*(7), 1279–1289.

Fagnani, F., & Zampieri, S. (2004). Quantized stabilization of linear systems: Complexity versus performance. *IEEE Transactions on Automatic Control*, *49*(9), 1534–1548.

Freudenberg, J. S., Middleton, R. H., & Solo, V. (2006). The minimal signal-to-noise ratio required to stabilize over a noisy channel. In *Proc. Amer. contr. conf.* (pp. 650–655).

Gersho, A., & Gray, R. M. (1993). *Vector quantization and signal compression*. Kluwer.

Goodman, D. J., & Gersho, A. (1974). Theory of an adaptive quantizer. *IEEE Transactions on Communications*, *22*, 1037–1045.

Goodman, D. J., & Wilkinson, R. M. (1975). A robust adaptive quantizer. *IEEE Transactions on Communications*, 1362–1365.

Graf, S., & Luschgy, H. (2000). *Foundations of quantization for probability distributions*. Springer.

Horn, R. A., & Johnson, C. R. (1985). *Matrix analysis*. Cambridge University Press.

Ishii, H., & Francis, B. A. (2003). Quadratic stabilization of sampled-data systems with quantization. *Automatica*, *39*(10), 1793–1800.

Kameneva, T., & Nesic, D. (2009). Robustness of quantized control systems with mismatch between coder/decoder initializations. *Automatica*,.

Kieffer, J. C. (1982). Stochastic stability for feedback quantization schemes. *IEEE Transactions on Information Theory*, *28*, 248–254.

Li, K., & Baillieul, J. (2004). Robust quantization for digital finite communication bandwidth (DFCB) control. *IEEE Transactions on Automatic Control*, *49*(9), 1573–1597.

Li, K., & Baillieul, J. (2007). Robust and efficient quantization and coding for control of multidimensional linear systems under data rate constraints. *International Journal of Robust and Nonlinear Control*, *17*, 898–920.

Liberzon, D. (2003). On stabilization of linear systems with limited information. *IEEE Transactions on Automatic Control*, *48*(2), 304–307.

Liberzon, D., & Nesic, D. (2007). Input-to-state stabilization of linear systems with quantized state measurements. *IEEE Transactions on Automatic Control*, *52*, 767–781.

Matveev, A. S., & Savkin, A. V. (2007a). An analogue of Shannon information theory for detection and stabilization via noisy discrete communication channels. *SIAM Journal on Control and Optimization*, *46*(4), 1323–1367.

Matveev, A. S., & Savkin, A. V. (2007b). Shannon zero error capacity in the problems of state estimation and stabilization via noisy communication channels. *International Journal of Control*, *80*, 241–255.

Nair, G. N., & Evans, R. J. (2004). Stabilizability of stochastic linear systems with finite feedback data rates. *SIAM Journal on Control and Optimization*, *43*(2), 413–436.

Wong, W. S., & Brockett, R. W. (1999). Systems with finite communication bandwidth constraints II: Stabilization with limited information feedback. *IEEE Transactions on Automatic Control*, *44*, 1049–1053.

Assaf Gurt was born in Petach-Tikva, Israel, in 1978. He received the B.Sc. degree in electrical and electronic engineering from Holon Institute of Technology, Israel in 2005, and is presently working towards his Ph.D. in electrical and electronic engineering at the University of Melbourne, Australia. His research interests lie in the area of data rate limitations in stochastic control systems.

Girish N. Nair was born in Petaling Jaya, Malaysia. He obtained a B.E. (Elec., 1st class hons.) in 1994, B.Sc. (math.) in 1995, and Ph.D. (elec. eng.) in 2000, on scholarships from the Australian government and the University of Melbourne. He is currently an associate professor in the Department of Electrical and Electronic Engineering at the University of Melbourne and has also held visiting positions at the University of Padova, Italy and Boston University, USA. He has received several prizes, including the SIAM Outstanding Paper Prize 2006, the Best Theory Paper Prize at the UKACC Int. Conf. Control, Cambridge, 2000 and the L. R. East Medal in electrical engineering, 1994. His research interests lie in the intersection of communications, information theory and control. He serves as an associate editor for the SIAM Journal on Control and Optimization.

Please cite this article in press as: Gurt, A., & Nair, G. N. Internal stability of dynamic quantised control for stochastic linear plants. Automatica (2009), doi:10.1016/j.automatica.2009.02.016